Novel aqueous sol–gel preparation and characterization of barium M ferrite, $BaFe_{12}O_{19}$ fibres

R. C. PULLAR, M. D. TAYLOR, A. K. BHATTACHARYA
Centre for Catalytic Systems and Materials Engineering, Department of Engineering, University of Warwick, Coventry CV4 7AL, UK

Gel fibres of barium M ferrite, $BaFe_{12}O_{19}$, were blow spun from an aqueous inorganic sol and calcined at temperatures up to 1200 °C. The ceramic fibres were shown by X-ray diffraction to be single phase crystalline M ferrite at 1000 °C, and surface area and porosity measurements indicated an unusually high degree of sintering at this temperature. The fibres also demonstrated a favourable grain structure of less than 0.1 μm at this temperature and maintained a small grain size of less than 4 μm even up to 1200 °C, an important factor in the magnetic properties of this material.

1. Introduction

Barium ferrite (M ferrite), $BaFe_{12}O_{19}$, is a uniaxial ferrimagnetic compound with the hexagonal magnetoplumbite structure [1], in which the direction of magnetism is parallel to the *c*-axis [2]. Since the discovery of the high crystal anisotropy of M ferrite [3] it has become one of the most important permanent magnetic materials [4]. This is due to its mechanical and magnetic hardness, thermal stability well above the Curie temperature (450 °C) [5] and relatively low cost. The high resistivity, magnetic permeability and coercivity of M ferrite also make it a useful material in both magnetic cores for inductors and transformers [6] and linear microwave devices [7]. In addition powdered ferrite may be added to plastics or rubbers to produce plastoferrite composite magnets [8].

Common preparative methods used in industry include milling, hot pressing, rolling and extruding and also melting techniques [9]. These techniques produce polycrystalline material with a grain structure of ~ 1 μm, whereas the co-precipitation of metal salts has given particle sizes as low as 0.15 μm [10]. For a magnetically optimized crystallite a grain size of less than 1 μm is required [11], with 80% of the theoretical maximum coercivity being reported for grains of 0.1 μm [12]. In addition the microstructure is dependent on the particle size and homogeneity of the precursor material and sintering conditions [11, 13].

This work on M ferrite fibres is part of a programme to demonstrate how a number of refractory and effect fibres can be made by an aqueous sol–gel route. Fibrous forms of a ceramic material can be made stronger and often stiffer than the bulk ceramic [14], and this would be an immediate advantage if the M ferrite were used in large composite magnets. Hale [15] has reviewed the effects of composite phase geometry on material properties and it is apparent that the incorporation of a magnetic material in fibrous form would have many advantages. The practical consequences have been demonstrated by Goldberg [16] who showed that in special cases, short fibres of 50:1 aspect ratio give a 50 fold advantage in magnetic permeability over the same volume of material in non-fibrous form.

Sol–gel routes to inorganic fibre forms bring advantages in processing. The sol–gel technique provides a means for the fine scale mixing of multiple components at low temperatures, resulting in a more homogenous precursor. Consequently improved sintering rates at lower temperatures can be expected, leading to improved microstructure. The inconvenient increased shrinkage between gel and ceramic product is more acceptable in an inorganic fibre due to its virtually one-dimensional nature. Therefore, given the potential advantages in successfully producing a sol–gel based route for the spinning M ferrite fibres, such a process is investigated in this paper.

2. Experimental procedure

2.1. Sample preparation

An acid-peptized, halogen-stabilized iron(III)hydroxide sol (Fe : anion = 3 : 2) was doped with a stoichiometric amount of a barium salt, which had been previously dissolved into a solution with an organic chelating agent. Spinnability was conferred by the addition of a small amount of polyethylene oxide as a spinning aid, and the fibres were produced by a proprietary blow spinning process [17]. The resulting gel fibres were collected as random staple and stored in a circulating air oven at 110 °C. The gel fibres were heat treated in a muffle furnace, firstly being pre-fired to 400 °C at 200 °C per h to remove water and any residual organic compounds. The samples were then

0022–2461

further heat treated at 200 °C per h to 600, 800, 1000, 1100 and 1200 °C in a re-crystallized alumina vessel for 3 h.

2.2. Characterization

2.2.1. Photon correlation spectroscopy (PCS)

Particle size measurement of the sol above the 3 nm diameter range was measured on a Malvern Instruments Lo-C autosizer and series 7032 multi-8 correlator, using a 4 mW diode laser, operating at a wavelength of 670 nm.

2.2.2. Scanning electron microscopy (SEM)

Scanning electron micrographs and analysis of the morphology of the samples was performed using a Cambridge Instruments stereoscan 90 SEM operating at 15 kV. Conducting samples were prepared by gold sputtering the fibre specimens.

2.2.3. Surface area and porosity measurements

Surface areas and pore size distributions of the fibres were measured using a Micrometrics ASAP 2000 using N_2 as the adsorption gas. Samples were degassed at 300 °C for 6 h prior to analysis.

2.2.4. X-ray photoelectron spectrocopy (XPS)

The XPS analysis was performed using a Kratos XSAM 800 spectrometer fitted with a dual anode (Mg/Al) X-ray source and a multichannel detector. The spectrometer was calibrated using the $Ag3d^{5/2}$ line at 397.9 eV and the AgMVV line at 901.5 eV. AlK_α radiation (1486.6 eV) was the exciting source (120W) and spectra were collected in the high resolution mode (1.2 eV) and fixed analyser transmission (FAT). The Kratos DS800 software, running on a DEC PDP11/23 computer, was used for data acquisition and analysis.

2.2.5. X-ray fluorescene spectrometry (XRF)

The elemental composition of the samples was measured on a Philips PW2400 sequential X-ray spectrometer fitted with a rhodium target end window X-ray tube and Philips X-40 analytical software. The samples were analysed in the form of a fused bead, where 1 g of sample was fused with 10 g of lithium tetraborate flux at 1250 °C for 12 min and then cast to form a glass bead.

2.2.6. X-ray powder diffraction (XRD) measurement

X-ray powder diffraction patterns of the samples treated at various temperatures were recorded in the region of $2\theta = 10$–80° with a scanning speed of 0.25 ° per min on a Philips PW1710 diffractometer using CuK_α radiation with a nickel filter. The refined cell parameters were obtained using linear regression procedures applied to the measured peak positions of all the major reflections up to $2\theta = 90^\circ$ using Philips APD 1700 software. This software was also used to calculate the average size of the crystallites in a sample using the Scherrer equation:

$$D = K\lambda/h_{1/2}\,\mathrm{Cos}\,\theta \quad (1)$$

where D = average size of the crystallites, K = Scherrer constant (0.9×57.3), λ = wavelength of radiation (0.15405 nm), $h_{1/2}$ = peak width at half height and θ corresponds to the peak position.

3. Results and discussion

The preparation of a stable doped sol was achieved with difficulty, after experimentation with many combinations of various metal salts, acids and organic stabilizers. The sol stability and the resulting size of the sol particles is sensitive to the preparative techniques and conditions, and the PCS technique enabled us to measure and control to a certain extent the properties of the sol. The PCS data indicates that the average particle size in the doped iron(III) sol was 7.4 nm, with a polydispersity of 0.630. By volume distribution, the mean size was found to be 6.6 nm, with an upper limit of 40 nm and an average molecular weight of 5.6×10^4 amu. It must be considered that the technique is unable to detect particles below the 3 nm threshold, and therefore these measurements may be higher than the actual true figures.

The dried fibre was strong and could be easily manipulated becoming slightly less so above 1000 °C but remaining tough enough to handle even up to 1200 °C. The fibres were very smooth and still fibrous with a diameter of 3–5 μm at 1000 °C. The grain size was beyond the resolution of the SEM, thus being below the 0.1 μm level, and no pores were visible (Fig. 1). At 1100 °C individual grains of size 0.5–2 μm could be seen, but the fibres had maintained their shape (Fig. 2), however by 1200 °C large plates up to 1–4 μm in diameter had formed, and the material had started to lose its fibrous nature. Commercial

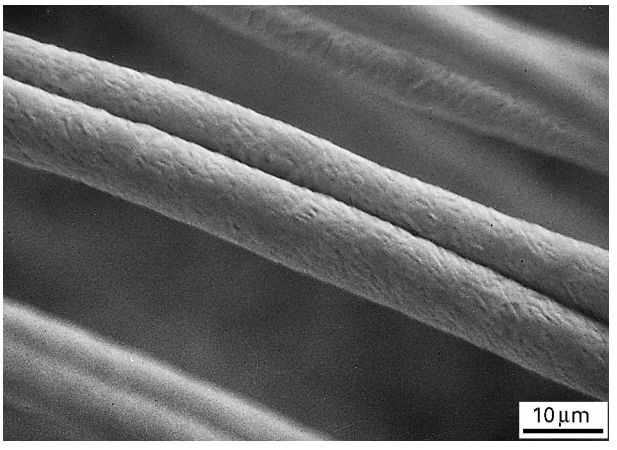

Figure 1 SEM micrograph of a pair of fibres fired to 1000 °C for 3 h.

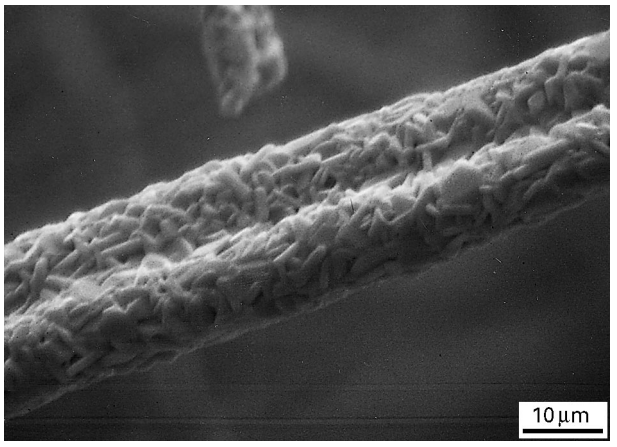

Figure 2 SEM micrograph of a pair of fibres fired to 1100 °C for 3 h.

M ferrite specimens show a grain size of 1–5 μm at 1000 °C and an exaggerated growth of 5–15 μm at 1225 °C [18]. Therefore the fibrous M ferrite appears to have a much reduced grain size as compared to standard powder mixes at equivalent temperatures, and the magnetic properties may thus be enhanced accordingly. Surface area and porosity data on the fibre fired to 1000 °C agreed with this, giving a low surface area ($0.9\,m^2\,g^{-1}$) and little porosity ($0.004\,cm^3\,g^{-1}$), with an average pore diameter of 53 nm.

A deviation in either the stoichiometry or oxidation state of the material can have an adverse effect on its magnetic properties [19], thus it is important to investigate these properties. The XPS analysis of the fibres fired to 1000 °C showed the oxidation state of the iron to be Fe(III) with a binding energy of 710.5 eV for the main Fe2p peak. The XRF elemental analysis for the oxides BaO and Fe_2O_3 confirmed the composition to be $BaFe_{12}O_{19}$ at 1000 °C, and all the halides had been lost by this temperature.

The XRD patterns taken between 400–1200 °C are shown in Fig. 3(a–e). Hematite has started to form by 400 °C (Fig. 3a), and by 600 °C it has fully crystallised (Fig. 3b) from the amorphous background matter. At 800 °C M ferrite has stared to form, with hematite still being the major phase (Fig. 3c), although by 1000 °C the sample is completely single phase M ferrite (Fig. 3d) and no further change in phase occurs up to 1200 °C (Fig. 3e). This agrees with previous studies on the reaction kinetics of hexaferrite formation, with M ferrite starting to form above 735 °C [20], and becoming a major phase by 1000 °C [21], although it is normally commercially sintered at the higher temperatures of 1200–1250 °C for several hours [22] to achieve sufficient densification. The average crystallite size was estimated to be 60 nm at 1000 °C, using the Scherrer equation on the 100% peak at $2\theta = 34.14°$.

4. Conclusions

A gel fibre was successfully spun from a doped iron(III) sol, which on subsequent heat treatment produced fully crystalline single phase M ferrite at 1000 °C. Although the ferrite did not appear to form at a significantly lower temperature, it did appear to be more fully sintered and with a much improved microstructure at equivalent temperatures than in conventionally manufactured specimens. As the magnetic properties may be enhanced accordingly, a further investigation is currently being carried out into the magnetic and structural properties of these fibres.

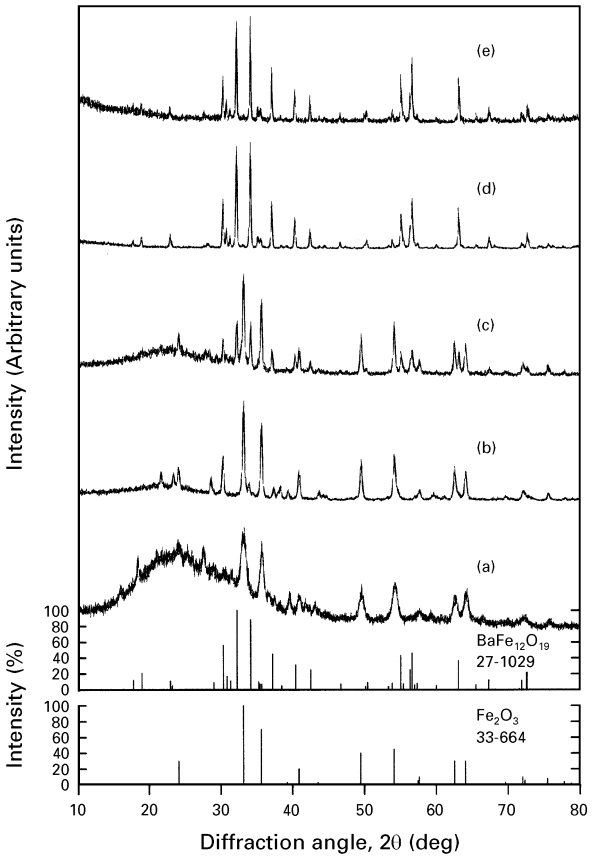

Figure 3 XRD patterns of the fibres fired to (a) 400 °C, (b) 600 °C, (c) 800 °C, (d) 1000 °C and (e) 1200 °C. For comparison purposes the JCPDS cards for Fe_2O_3 no 33-664 and $BaFe_{12}O_{19}$ no 27-1029 are also displayed.

Acknowledgements

Our thanks to D. Croci for surface area and porosity measurements, R. C. Reynolds for the XPS and XRD characterization, K. K. Mallick for XRD characterization (all at the Centre for Catalytic Systems and Materials Engineering, Department of Engineering, University of Warwick) and R. Burton for the XRF analysis (Materials Research Institute, Sheffield Hallam University).

References

1. V. ADELSKOLD, *Arkiv. Kemi., Min. Geol.* **12A** (1938) 1.
2. G. H. JONKER, H .P. WIJN and P. B. BRAUN, *Phil. Techn. Rev.* **18** (1956) 145.
3. J. J. WENT, G. W. RATHENAU, E. W. GORTER and G. W. VAN OOSTERHAUT, *Phil. Techn. Rev.* **13** (1952) 194.
4. E. A. M. VAN DER BROEK and A. L. STUIJTS, *ibid* **37** (1977-8) 169.
5. H. STABLEIN, in "Ferromagnetic Materials" Vol. 3, edited by E. P Wohlfarth (North-Holland, Amsterdam, 1982) p. 448.

6. E. E. RICHES, in "Ferrites" (Mills and Boon Technical Library, London, 1972) p. 10.
7. W. H. VON AULOCK and C. E. FAY, in "Linear Ferrite Devices for Microwave Applications" (Academic Press, New York, 1968).
8. E. E. RICHES, in "Ferrites" (Mills and Boon Technical Library, London, 1972) p. 37.
9. H. STABLEIN, in "Ferromagnetic Materials" Vol. 3, edited by E. P Wohlfarth (North-Holland, Amsterdam, 1982) pp. 462–535.
10. H. HANEDA, Ch. MIYAKAWA and H. KOJIMA, *J. Amer. Ceram. Soc.* **57** (1974) 354.
11. H. G. RICHTER, *IEEE Trans.*, MAG-4 (1968) 263.
12. K. HANEDA and H. KOJIMA, *J. Appl. Phys.* **44** (1973) 3760.
13. R. L. COBLE, *J. Appl. Phys.* **32** (1961) 787.
14. A. KELLY, in "Strong Solids" (Clarendon Press, Oxford, 1973).
15. D. K. HALE, *J. Mater. Sci.* **11** (1976) 2105.
16. H. A. GOLDBERG, *US Pat*. 4725 490 (1973).
17. M. J. MORTON, J. D. BIRCHALL and J. E. CASSIDY, *UK Pat*. 1360 200 (1974).
18. H. STABLEIN, *Tech. Mitt. Krupp., Forsch.-Ber.* **26** (1968) 81.
19. J. SMIT and H. P. J. WIJN, in "Ferrites" (Philips Technical Library, Eindhoven, 1959) p. 221.
20. A. G. SADLER, *J. Can. Ceram. Soc.* **34** (1965) 155.
21. M. ERCHAK, I. FANKUCHEN and R. WARD, *J. Amer. Ceram. Soc.* **68** (1946) 2085 and 2093.
22. H. STABLEIN, in "Ferromagnetic Materials" Vol. 3, edited by E. P Wohlfarth (North-Holland, Amsterdam, 1982) pp. 505–7.

Received 19 April
and accepted 21 May 1996